Hindawi
Mathematical Problems in Engineering
Volume 2022, Article ID 2227811, 11 pages
https://doi.org/10.1155/2022/2227811

Research Article

Hybrid Methodology for the Computational Behaviour of Thermal Radiation and Chemical Reaction on Viscoelastic Nanofluid Flow

Pradyumna Kumar Pattnaik,[1] **Satya Ranjan Mishra**,[2] **S. Panda**,[3,4] **Shoeb Ahmed Syed**,[5] **and Kamalakanta Muduli**[5]

[1]*Department of Mathematics, Odisha University of Technology and Research, Bhubaneswar 751029, Odisha, India*
[2]*Department of Mathematics, Siksha 'O' Anusandhan University, Bhubaneswar 751030, Odisha, India*
[3]*Department of Mathematics, National Institute of Technology, Aizawl 796012, Mizoram, India*
[4]*Nalanda Institute of Technology, Chandaka, Bhubaneswar 754005, India*
[5]*Papua New Guinea University of Technology, Lae, Morobe, Papua New Guinea*

Correspondence should be addressed to Kamalakanta Muduli; kamalakanta.muduli@pnguot.ac.pg

Received 25 August 2022; Revised 27 September 2022; Accepted 28 September 2022; Published 11 October 2022

Academic Editor: Waleed Adel

Copyright © 2022 Pradyumna Kumar Pattnaik et al. This is an open access article distributed under the Creative Commons Attribution License, which permits unrestricted use, distribution, and reproduction in any medium, provided the original work is properly cited.

The current investigation carries out the free convection of an electrically conducting viscoelastic nanofluid through an expanding surface. The salient features of Brownian and thermophoresis due to cross-diffusion and thermal radiation enhance the heat transport phenomenon. Furthermore, the chemical reaction plays an important role in enriching the study. The current investigation shows its important role, such as the proper shape and size of the product in the final stage of production and also optimizing the transport phenomena of various industries that depend upon the supplied heat source, etc. With the appropriate selection of transformation rules, the proposed model is designed and transformed into the ordinary. Furthermore, a hybrid methodology such as the "*Perturbation Meth*od" and numerical technique, i.e., the "MATLAB solver (*bvp4c technique)*," is proposed to handle the governing equations. The graph and tabular form illustrate the characteristics of physical parameters blending within the flow phenomena.

1. Introduction

The combined significance of heat absorption/generation with a radiative effect on magnetohydrodynamic (MHD) free convection flow is important for numerous scientific, engineering, and industrial applications like high-temperature casting, furnace design, missiles, propulsion devices for aircraft, space vehicles, and satellites, etc. Choi [1] considered a nanofluid to enhance thermal conductivity and demonstrated this by imposing Hamilton and Crosser models for considering copper nanoparticles in the base fluid water. Takhar et al. [2] investigated the MHD flow properties of conducting liquid on a continuously expanding surface. Moreover, Azim and Chowdhury [3] studied the laminar MHD conjugate natural convection flow for Joule heating and internal heat generation on a horizontal circular cylinder.

The unsteady magnetohydrodynamics (MHD) natural convection of viscous fluid through the vertical permeable surface with the effect of the chemical species and radiative heat is studied by Parida et al. [4]. Numerous slips and the influence of reactive species on MHD heat transfer over an expanding sheet for the radiative effect were researched by Ramana et al. [5]. Suganya et al. [6] described a mathematical model of MHD free convection of viscous fluid in an inclined plane. In this study, the "*Modified Homotopy Perturbation Method*" was employed. Uddin et al. [7] inspected the role of mixed convection on MHD flow over the saturated permeable plate and handled it numerically following Runge-Kutta's sixth-order integration scheme. Sarada [8] considered unsteady MHD flow over a vertical surface saturated in the porous medium and the effect of chemical reaction, where the variation in suction velocity

varies with the same frequency as the plate temperature. Seth et al. [9] deliberated the magnetohydrodynamic flow phenomena of a rotating fluid over a vertical surface with wall temperature along the Hall current solving by the Laplace transform technique. The oscillatory MHD flow in an irregular channel for the impact of the source, chemical reactions, and the radiative effect was researched by Narayana et al. [10]. Reddy et al. [11] proposed that the impact of chemical reactions and thermal radiation through a vertical plate on unsteady free convection saturated within a permeable medium be discussed. The terminologies for the governing parameter distributions are numerically explained by the "*fourth-order Runge-Kutta method*" and the shooting technique. Ahmed and Das [12] investigated the free convection effect on an inclined plate surrounded by a porous medium and the effect of a chemical reaction. A uniform magnetic field is presumed to be applied normally to the plate as it is absorbed into the fluid region. Raju et al. [13] carefully investigated a time-independent MHD convective flow of viscous fluid through a horizontal conduit in which the bottom wall is impermeable, and they imposed the behaviour of dissipative heat conditions.

Moreover, Mondal et al. [14] analyzed the illustration of cross-diffusion and convective boundary conditions through an inclined plate for the behaviour of source/sink and chemical reactions. Sehra et al. [15] described the free convection of a conducting viscous fluid flow with the impact of molecular diffusivity over a plate placed normal to the flow, as well as the time-dependent shear stress and exponential heat source. Agbaje and Leach [16] explored an unsteady MHD convective flow for the consequences of a heat source and radiation, which was solved numerically by the spectral Perturbation Method. Khan and Naz [17] examined the 3D flow of heat transport properties of a second-grade liquid embedded in a porous medium considering an expanding wall, and further, they proposed the "Homotopy Analysis Method." Moreover, Rajagopal et al. [18] described unsteady 3D magnetohydrodynamic flow over a stretching sheet through a permeable medium based on impulsive motion. Many researchers [19–29] have contributed their valuable research ideas in the MHD flow field with different novelty methods used to tackle the PDEs through the Laplace transform method. However, various transformations are proposed to convert PDEs to ODEs and then solved using numerical techniques, such as 4^{th} order RK-Method by deploying shooting technique, MATLAB inbuilt software bvp4C/bvp5C/finite difference method, etc. Some of their works follow other analytical methods like the "Adomian Decomposition Method," "Differential Transform Method," etc.

Biswas et al. [30] reported on a two-dimensional Maxwell magnetohydrodynamics nanofluid across an extended sheet regarding thermal radiation and chemical reactions. In this literature survey, the fluid velocity enlarges for the parameters' boosted values. Furthermore, streamlines and isotherms have been evaluated for the multiple parametric values. Zeb et al. [31] deliberated the Eyring-Powel ferrofluid with the addition of thermal radiative effect and magnetic dipole along with chemical reaction subjected to heterogeneous and homogeneous situations over a stretchable surface computed via the Runge-Kutta method with shooting procedure. Javid et al. [32] examined the physical impacts of electro-osmosis and magnetic fields embedded in porosity and thermal slip-on flow on nanofluid via an asymmetric microchannel accomplished with convective boundary conditions. Aldabesh et al. [33] researched the features of Darcy resistance and Arrhenius activation energy on the aspect of a nanofluid occupied with microorganisms via an extended cylinder. This survey is also protracted by applying modified Fourier and Fick's theories. Raza et al. [34] considered the significance of a slip boundary wall and magnetized field over an inclined plate by implementing fractional derivatives obtained through the Laplace transformation scheme. Khan et al. [35] deliberated magnetized couple stress nanoparticles with the features of numerous factors proficient with the Buongiorno model, which is simulated by homotopy procedures. Haq et al. [36] examined the laminated flow of hybrid nano-liquids considering effective nanoparticles with the features of Joule heating as well as the Darcy-Forchheimer effect computed by the Mathematica tool. Alharbi et al. [37] explored the flow of hybrid nanofluid subjected to single-walled and multi-walled carbon nanotubes with the structures of the Brinkman-type fluid model. Khan et al. [38] were concerned with the Atangana-Baleanu Caputo fractional derivative and its characteristics. A fixed-point scheme has been used to find the uniqueness and existence of solutions for the fractional DSEK model. Higazy et al. [39] investigated the optimal control of deadly lassa hemorrhagic fever disease in pregnant women; furthermore, numerically simulated by the Laplace transform and the Adomian Decomposition Method.

The earlier literature provides the gateway to investigating the free convection of viscoelastic nanofluid through an expanding surface. The electrically conducting liquid for the interaction of magnetic properties, the role of radiative heat, and the chemical species significantly augment the flow phenomena. As a novelty, the present model is handled by hybridising analytic technique such as the Perturbation Method and partially solved by numerical techniques. The computation is carried out using the in-house computational software MATLAB and its built-in function bvp4c. Furthermore, compared with the prior investigation, the computational results show a good agreement in particular cases.

Based upon the discussion described above, the following research questions arise:

(i) What happens if we consider a single-phase model instead of a two-phase model nanofluid?

(ii) Whether the use of hybrid nanofluid or ternary nanofluid in the proposed study will perform a Newtonian or non-Newtonian fluid?

(iii) Which nanoparticles, i.e. consideration of metal, oxides, carbides, and CNT, will be valid for the current viscoelastic fluid?

(iv) Will the shape and size of various nanoparticles affect the viscoelastic nanofluid past a stretching surface?

(e) Whether consideration of free stream boundary condition affects the flow phenomena of the proposed problem?

2. Basic Equations

The natural convection of an incompressible non-Newtonian laminar flow of a nanofluid based on the Buongiorno model through an expanding sheet is proposed in this investigation. The stretching sheet velocity is assumed to be $U = cx$ with the rate constant $c(>0)$. Furthermore, the temperature-dependent heat source is proposed as a novelty of the study to examine the impact of the difference between the temperature of the surface and the ambient state. The flow is scheduled to move along the direction of the sheet, i.e. the x-axis, and the y-axis is placed in the normal direction of the flow. The magnetized fluid affects the flow properties because of the magnetic field of strength B_0 (Figure 1). Moreover, the fluid temperature and concentration at the surface are T_w, C_w and whereas the ambient state conditions are T_∞ and C_∞ successively. Moreover, the thermal equilibrium state is maintained for both the fluid and nanoparticle phases. Therefore, with the proposed conditions assumed in the present investigation, the governing equations are as follows:

$$\frac{\partial u}{\partial x} + \frac{\partial v}{\partial y} = 0, \tag{1}$$

$$u\frac{\partial u}{\partial x} + v\frac{\partial v}{\partial y} = v\frac{\partial^2 u}{\partial y^2} + \frac{\alpha_1}{\rho_f}\left[\frac{\partial u}{\partial x}\frac{\partial^2 u}{\partial y^2} + u\frac{\partial^3 u}{\partial x\,\partial y^2} + \frac{\partial u}{\partial y}\frac{\partial^2 v}{\partial y^2} + v\frac{\partial^3 u}{\partial y^3}\right] - \frac{\sigma}{\rho_f}B_0^2 u + g\beta_T(T - T_\infty) + g\beta_c(C - C_\infty), \tag{2}$$

$$u\frac{\partial T}{\partial x} + v\frac{\partial T}{\partial y} = \alpha_m\nabla^2 T + \tau\left[D_B\frac{\partial C}{\partial y}.\frac{\partial T}{\partial y} + \frac{D_T}{T_\infty}\left(\frac{\partial T}{\partial y}\right)^2\right] + \frac{Q_0}{(\rho c_p)_f}(T - T_\infty) - \frac{1}{(\rho c_p)_f}\frac{\partial q_r}{\partial y}, \tag{3}$$

$$u\frac{\partial C}{\partial x} + v\frac{\partial C}{\partial y} = D_B\frac{\partial^2 C}{\partial y^2} + \frac{D_T}{T_\infty}\frac{\partial^2 T}{\partial y^2} - K_c^*(C - C_\infty). \tag{4}$$

where u and v are presented successively as the velocity components directed along the x and y axes; here, p is denoted as pressure ρ_f, ρ_p, the fluid and particle densities, μ the fluid viscosity v, the kinematic viscosity σ, the electrical conductivity, α_1 the material parameter B_0, the magnetic strength, T, the fluid temperature, α_m the thermal diffusivity $\tau = (\rho c_p)_p/(\rho c_p)_f$, the heat capacity ratio, C volume fraction, D_B and D_T, the Brownian and thermophoresis T_∞, the free stream temperature, c_p the specific heat, and g, k is the gravitational force and the thermal conductivity. The term $Q_0(T - T_\infty)$ is heat generation or absorption. In this particular case, the wall temperature $T > T_\infty$, the source is expressed as $Q_0 > 0$ and the heat sink is expressed as $Q_0 < 0$.

The following assumed boundary conditions are given:

$$\left.\begin{aligned} &u = U + \kappa v\frac{\partial u}{\partial y}, v = 0, T = T_w, C = C_w, \text{ at } y = 0 \\ &u \longrightarrow 0,\ T \longrightarrow T_\infty,\ C \longrightarrow C_\infty \text{ as } y \longrightarrow \infty \end{aligned}\right\}. \tag{5}$$

The proposed governing equations are transformed to their nondimensional form by the assumption of the following rule:

$$\eta = \sqrt{\frac{c}{v}}y, u = cxf'(\eta), v = -\sqrt{cv}f(\eta), \theta(\eta) = \frac{T - T_\infty}{T_w - T_\infty},$$
$$\phi(\eta) = \frac{C - C_\infty}{C_w - C_\infty}. \tag{6}$$

The transformed equations, along with the boundary conditions, are as follows:

$$f''' + ff'' - f'^2 - Rc\left(f''^2 - 2f'f''' + ff^{iv}\right) - Mf' + \lambda_1\theta + \lambda_2\phi = 0, \tag{7}$$

$$\frac{1}{\Pr}(1 + Nr)\theta'' + f\theta' + Nb\,\theta'\phi' + Nt\,\theta'^2 + Q\theta = 0, \tag{8}$$

$$\frac{1}{Le\Pr}\phi'' + f\phi' + \frac{Nt}{Nb}\frac{1}{Le\Pr}\theta'' - Kc\phi = 0, \tag{9}$$

$$\left.\begin{aligned} &f(0) = 0, f'(0) = 1 + K f''(0), \theta(0) = 1, \phi(0) = 1, \\ &f'(\infty) \longrightarrow 0,\ \theta(\infty) \longrightarrow 0,\ \phi(\infty) \longrightarrow 0 \end{aligned}\right\}, \tag{10}$$

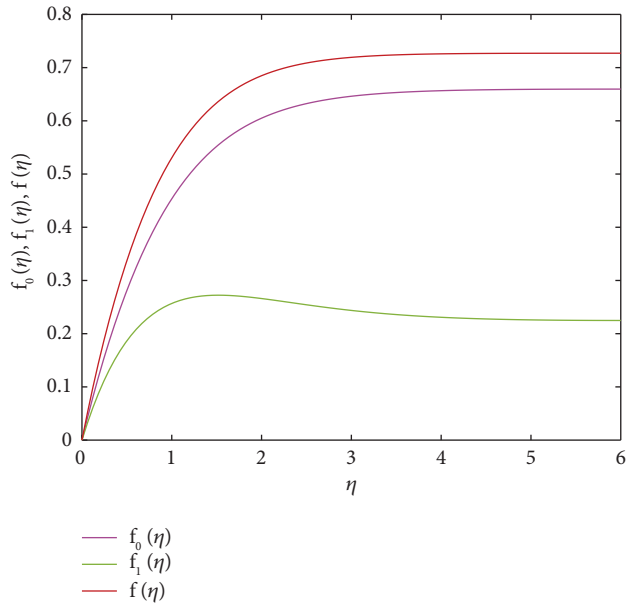

Figure 1: Flow geometry.

where the prime presents the differentiation in respect of η concerning, and the dimensionless parameters are as follows:

$$Rc = \frac{\alpha_1 c}{\mu}, M = \frac{\sigma B_0^2}{\rho_f c}, Gr_x = \frac{g\beta_T (T_w - T_E)x^3}{\upsilon^2}, \lambda_1 = \frac{Gr_x}{\mathrm{Re}_x^2}, Gc_x = \frac{g\beta_T (C_w - C_E)x^3}{\upsilon^2}, \lambda_2 = \frac{Gc_x}{\mathrm{Re}_x^2}, \mathrm{Pr} = \frac{\upsilon}{\alpha_m},$$

$$Nr = \frac{16\sigma^* T_E^3}{3(\rho c_p)_f \kappa \upsilon}, Nb = \frac{(\rho c_p)_p D_B (C_w - C_E)}{(\rho c_p)_f \upsilon}, Nt = \frac{(\rho c_p)_p D_T (T_w - T_E)}{(\rho c_p)_f T_E \upsilon}, Q = \frac{Q_0}{c(\rho c_p)_f}, K = \kappa\sqrt{c\upsilon}, \tag{11}$$

$$Le = \frac{\alpha_m}{D_B}, Kc = \frac{K_c^*}{c}.$$

Here, Pr is the Prandtl number; Le, the Lewis number; M, the magnetic parameter; α, the viscoelastic parameter; the Q, heat source/sink parameter; Nb, Brownian motion; and Nt, the thermophoresis parameter, respectively.

3. Hybridization of Perturbation Method and Numerical Method (bvp4c)

The Perturbation Method is used first to reduce the highest order derivative of the momentum equation, which results in two differential equations. The numerical method bvp4c, an inbuilt code in the MATLAB software, was then used for computation and drawing graphs.

3.1. Perturbation Method. Introducing $f = f_0 + Rc f_1 + O(Rc^2)$ in (7) and equating the coefficients of Rc^0 and Rc^1, one can get with proposed boundary conditions,

$$f_0''' + f_0 f_0'' - M f_0' - \dot{f_0^2} + \lambda_1 \theta + \lambda_2 \phi = 0, \tag{12}$$

$$f_1''' + f_0 f_1'' + f_1 f_0' - 2 f_0' f_1' - \left(f_0'' - 2 f_0' f_0''' + f_0 f_0^{iv}\right) - M f_1' = 0. \tag{13}$$

$$\left.\begin{array}{l} f_0(0) = 0, f_0'(0) = 1 + K f_0''(0), \\ f_1(0) = 0, f_1'(0) = K f_1''(0), \\ f_0'(\infty) \longrightarrow 0, f_1'(\infty) \longrightarrow 0, \theta(\infty) \longrightarrow 0, \phi(\infty) \longrightarrow 0. \end{array}\right\}, \theta(0) = 1, \phi(0) = 1, \tag{14}$$

3.2. Numerical Method. All the perturbed equations (11)–(13), along with temperature and concentration (8) and (9), are now discretized. All these above equations with the boundary conditions are converted into a set of 1st order ODEs as follows:

$$
\begin{aligned}
&f_0 = y_1, f_0' = y_2, f_0'' = y_3, f_1 = y_4, f_1' = y_5, f_1'' = y_6, \theta = y_7, \theta' = y_8, \phi = y_9, \phi' = y_{10},\\
&f_0''' = -y_1 y_3 + M\, y_2 + y_2^2 - \lambda_1 y_7 - \lambda_2 y_9,\\
&f_1''' = \begin{cases} -y_1 y_6 - y_4 y_3 + 2y_2 y_5 + y_3^2 - 2y_2\left(-y_1 y_3 + M\, y_2 + y_2^2 - \lambda_1 y_7 - \lambda_2 y_9\right) \\ +y_1 * di\ ff\left(-y_1 y_3 + M\, y_2 + y_2^2 - \lambda_1 y_7 - \lambda_2 y_9\right) + M\, y_5 \end{cases}\\
&\theta'' = \Pr\left(-(y_1 + Rc\, y_4) y_8 - Nb\, y_8 y_{10} - Nt\, y_8^2 - Q\, y_7\right)/(1 + Nr)\\
&\phi'' = Le\Pr\left(-(y_1 + Rc y_4) y_{10} + \frac{Nt}{Nb}\frac{1}{Le(1+Nr)}\left((y_1 + Rc\, y_4) y_8 + Nb\, y_8 y_{10} + Nt\, y_8^2 + Q\, y_7\right) + Kc\, y_9\right)
\end{aligned}
\tag{15}
$$

$$
y_1(0) = 0, y_2(0) - 1 - K\, y_3(0) = 0, y_4(0) = 0, y_5(0) - K\, y_6(0) = 0, y_7(0) - 1 = 0, y_9(0) - 1 = 0,
$$

$$
y_2(\infty) \longrightarrow 0, y_5(\infty) \longrightarrow 0, y_7(\infty) \longrightarrow 0, y_9(\infty) \longrightarrow 0.
$$

All these calculations had to be carried out using the MATLAB package. This program is run with step size $\eta = 0.01$ and $\eta_\infty = 6$ solved in intervals $0 \le \eta \le \eta_\infty$. The numerical steps for bvp4c are as follows:

(i) The nonlinear PDE is a first-order ordinary differential equation

(ii) Bvp4c returns the solution as a structure named sol

(iii) mesh selection is generated and returned in the sol.x field

(iv) The solution can be obtained from the array sol.y corresponding to sol.x

(v) $y(0)$ was adopted as the left limit and y_∞ was adopted as the right limit

4. Physical Quantities of Engineering Interests

The rate coefficients, i.e., shear rate coefficient (Cf_x), local Nusselt number (Nu_x), and Sherwood number (Sh_x), are described as follows:

$$
Cf_x = -\frac{2\tau_w}{\rho u_w^2}, Nu_x = -\frac{x q_w}{k(T_w - T_\infty)}, Sh_x = -\frac{x j_w}{D_B(C_w - C_\infty)}. \tag{16}
$$

In the above expressions, τ_w, q_w and j_w are defined as follows:

$$
\tau_w = \mu\left(\frac{\partial u}{\partial y}\right)_{y=0} + \alpha_1\left(u\frac{\partial^2 u}{\partial x\, \partial y} - 2\frac{\partial u}{\partial x}\frac{\partial u}{\partial y}\right)_{y=0}, q_w = -\left(\frac{16\sigma^* T^3}{3k^*} + k\right)\left(\frac{\partial T}{\partial y}\right)_{y=0}, j_w = -D_B\left(\frac{\partial C}{\partial y}\right)_{y=0}, \tag{17}
$$

where τ_w denotes the shear stress, q_w wall heat flux j_w, wall mass flux and k thermal conductivity of the nanofluid with $\mathrm{Re}_x = cx^2/\nu$ Reynolds number. The nondimensional forms are as follows:

$$
Cf_x \mathrm{Re}_x^{0.5} = \left(1 + 3Rc\, f'(0)\right) f''(0), \tag{18}
$$

$$
\mathrm{Re}_x^{0.5} Nu_x = -(1 + Nr)\theta'(0), \tag{19}
$$

$$
\mathrm{Re}_x^{0.5} Sh_x = -\phi'(0). \tag{20}
$$

5. The Physical Significance of Parameters

As a need of recent technology and the use of several electronic gadgets in daily requirement objects, it is seen that the proposed solution is very useful. Therefore, concentrating on the current requirement, our objective is to analyze the free convection of the non-Newtonian nanofluid through a vertical expanding surface for the conjunction of several physical quantities because of the cross-diffusion of the profiles; the appearance of Brownian and thermophoresis play a vital role in this study. Furthermore, the radiative heat and the chemical reaction significantly encourage the flow profiles. The proposed model was transformed into a set of equations and further solved by employing a hybrid methodology that combines analytical and numerical methods. Because of the unavailability of sufficient boundary conditions, the velocity profile is perturbed by considering a perturb parameter, and then the set of momentum equations along with the energy and solutal profiles are solved numerically. To check the validity and convergence of the proposed methodologies, the present results of the heat transfer rate profiles are compared with the earlier published results. In particular situations, the results validate the work of Khan and Pop [40] and Gorla and Sidawi [41], which are presented in Table 1, and show a good agreement.

Moreover, the other characterizing parameters and their physical significance are deployed graphically and displayed

Table 1: Comparison of rates of heat transfer.

Pr	$-\theta'(0)$		
	Khan and Pop [40]	Gorla and Sidawi [41]	Present
0.2	0.1691	0.1691	0.169346
0.7	0.4539	0.4539	0.4538751
2	0.9113	0.9114	0.9113956

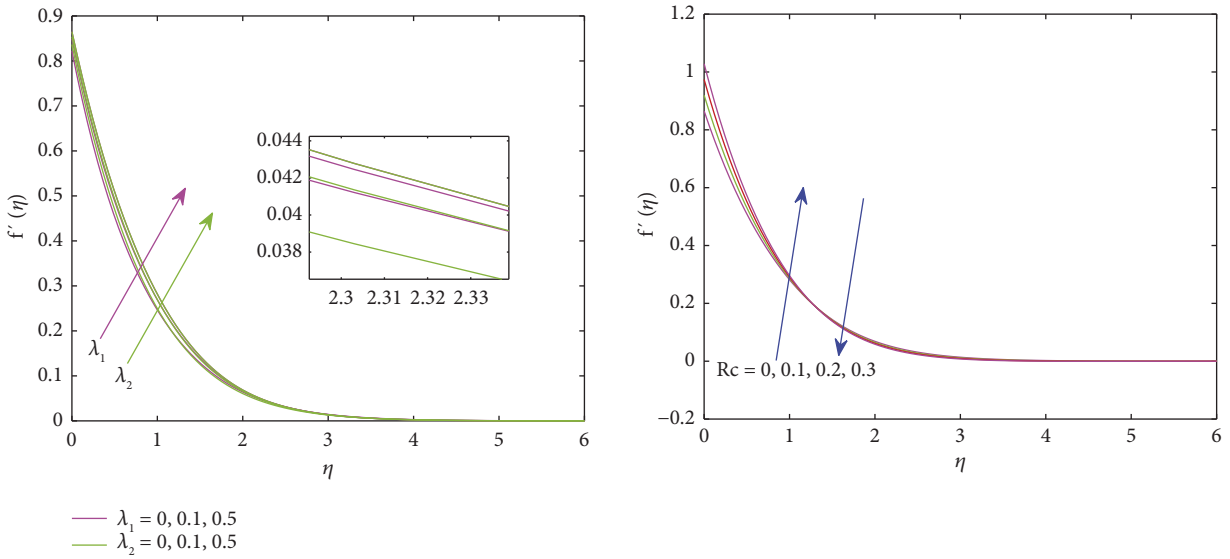

Figure 2: Behaviour comparison of zeroth, first order, and final stream function.

in tabular form for the rate coefficients. The computational process is obtained from the fixed values of the following parameters: $Rc = 0.3, M = 1, \lambda_1 = 0.5, \lambda_2 = 0.5, Pr = 7, Nr = 0.5, Nb = 0.5, Nt = 0.01, Q = 0.01, K = 0.5, Le = 1$, and $Kc = 1$. Figure 2 illustrates the velocity profiles in several perturbation cases like the zeroth and first order; furthermore, the entire profile is also deployed. This behaviour characterizes the significant role of the perturb parameters, and it was concluded that the profile became smooth in the final stage solution of the entire profiles of velocity distribution.

Figure 3 illustrates the role of the elasticity constraint Rc on the velocity distribution. The several values of Rc, i.e., $Rc = 0$ suggest the Newtonian characteristics and $Rc \neq 0$ indicate the non-Newtonian behaviour, i.e., the significant features of the viscoelastic parameter on the fluid velocity profile. The Newtonian nanofluid exhibits a thinner bounding surface thickness near the sheet. Furthermore, the non-Newtonian fluid, i.e., an increasing viscoelastic parameter, encourages the velocity profiles within the domain $\eta < 1$, and afterwards, a reverse trend is exhibited with insignificant characteristics to reach the boundary conditions. Figure 4 portrays the physical properties of the inclusion of magnetic parameters along with the velocity slip on the nanofluid velocity distribution. The conjunction of the magnetic field experiences a resistive force, which produces a Lorentz force, which discourages the fluid velocity from moving up. Therefore, increasing the magnetic parameter resists the velocity within the domain. The opposing character of the magnetic parameter may be beneficial for manufacturing numerous engineering goods for their better shape and size. Moreover, the nonoccurrence of the magnetic parameter exhibits a greater thickness of the profiles in comparison to the inclusion of the magnetic parameter. The same figure exhibits the role of velocity slip on the nanofluid velocity. Here, the slip parameter K ($K = 0$) signifies the no-slip condition, i.e., the velocity at the sheet became constant, and further $K \neq 0$ indicates the role of slip on the momentum profile. The observation reveals that the enhanced slip parameter decelerates the flow profiles with an asymptotic profile trend. This nature exhibits a thinner bounding surface near the sheet region, and afterward, an insignificant reverse trend is illustrated. Figure 5 displays the impact of buoyancy parameters, i.e., the role of both thermal and solutal buoyancy parameters on the nanofluid velocity. The pressure differential between the fluid layers causes the buoyancy force when the particle is submerged into the fluid. The pressure generated on the upper layer is dominated by the pressure at the bottom, exhibiting an upward force for which the fluid velocity enhances the increasing buoyancy parameters. In the absence of free convection, the bounding surface thickness diminishes significantly. The significant characteristics of the several parameters affecting the fluid temperature are displayed and elaborated.

Figure 6 describes the characteristics of the elasticity parameter and the velocity slip affecting the fluid temperature. The enhanced property of the viscoelastic parameter retards the nanofluid temperature, whereas a reverse trend is

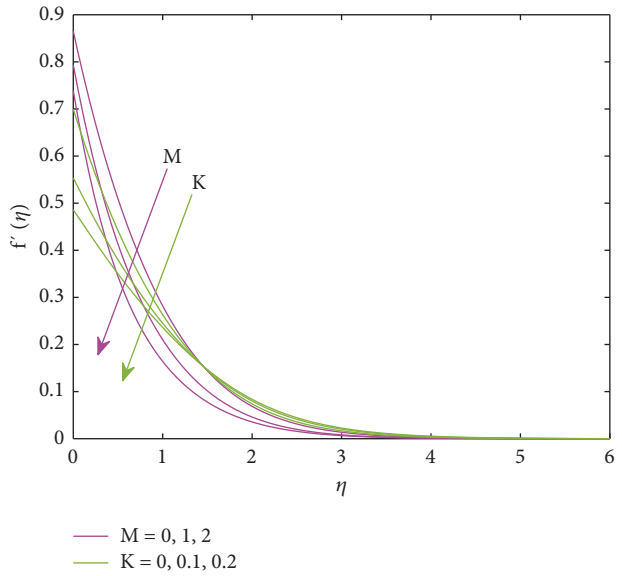

Figure 3: Role of *Rc* on fluid velocity.

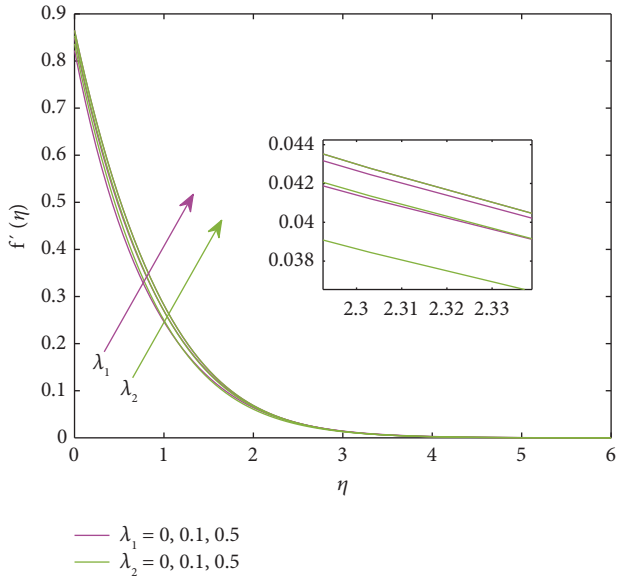

Figure 4: Role of *M* and *K* on fluid velocity.

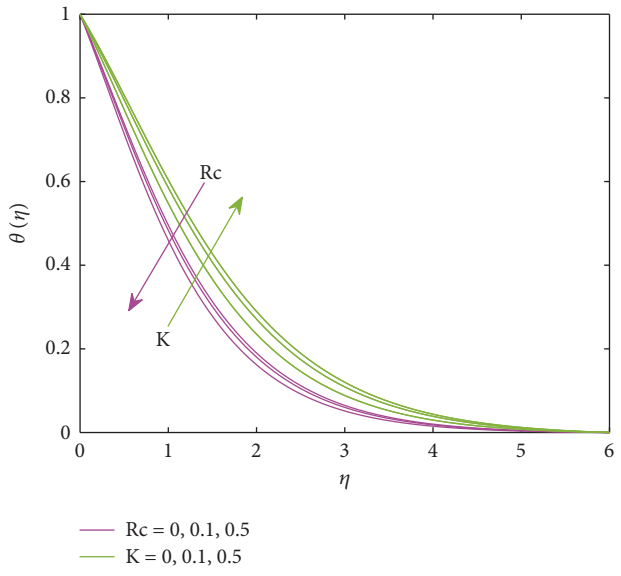

Figure 5: Role of λ_1 and λ_2 on fluid velocity.

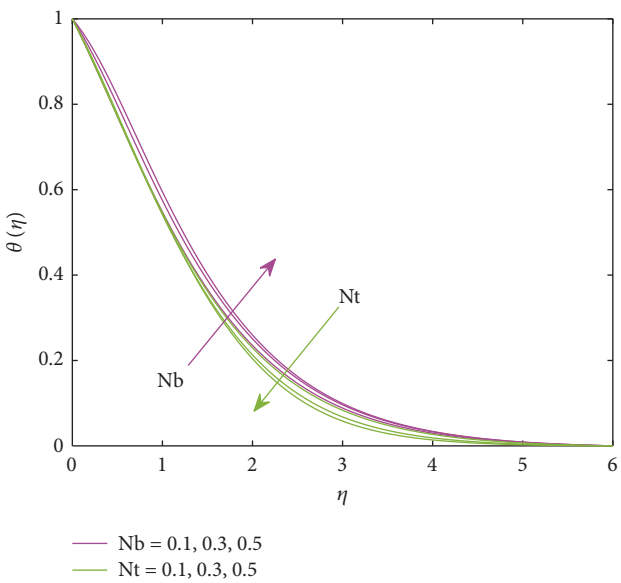

Figure 6: Behavior of *K* and *Rc* on fluid temperature.

exhibited for the augmentation in the velocity slip. In the case of a constant fluid velocity at the sheet region, the surface thickness lowers significantly. The case of Newtonian fluid exhibits maximum velocity when compared to elastic fluid. Figure 7 exhibits the variation of Brownian and thermophoresis on the fluid temperature due to the cross-diffusion effect. Brownian motion occurs due to the particles' arbitrary or random motion and collisions with the surroundings and the molecules. The interaction of the concentration gradient induces these particles. Though this movement occurs from the area of high concentration to the area of low concentration, the increasing Brownian motion boosts the temperature profile. Further, thermophoresis experiences a force created due to the temperature gradient between the hot gas and the cold wall. Therefore, augmentation in the thermophoresis parameter retards the fluid temperature, exhibiting the thermal bounding surface thickness thinning. Figure 8 characterizes the behaviour of the supplementary heat source and the radiating heat on the nanofluid temperature distribution. The radiative heat deals with the release of electromagnetic radiation obtained from the particles present in the liquid. This transfers the amount of electromagnetic radiation known to be thermal radiation. The enhanced thermal radiation overshoots the temperature profile, enhancing surface thickness. The growth in heat sources also encourages temperature distributions to vary significantly. Figure 9 demonstrates the behaviour of the Brownian and thermophoresis parameters on the nanofluid

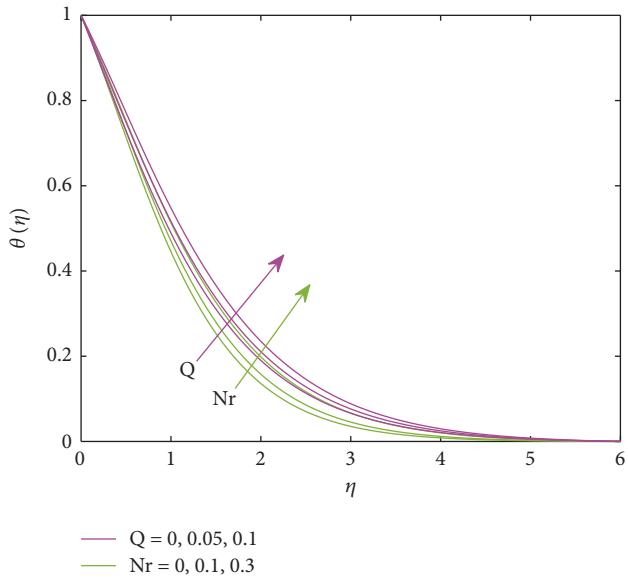

Figure 7: Behavior of Nb and Nt on fluid temperature.

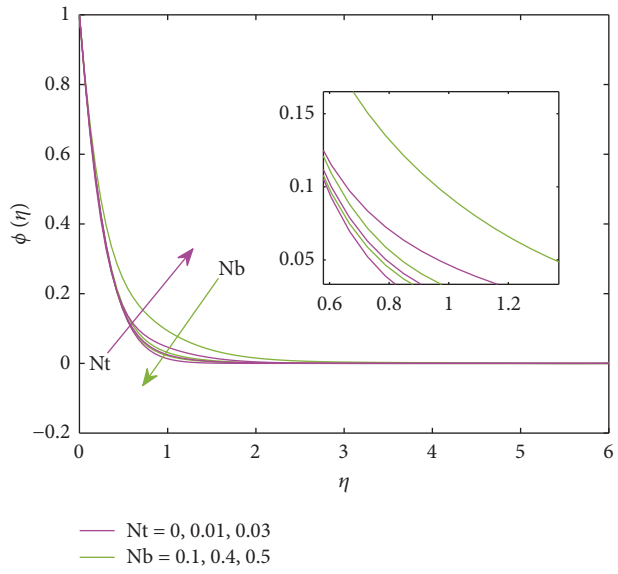

Figure 9: Role of Nb and Nt on fluid concentration.

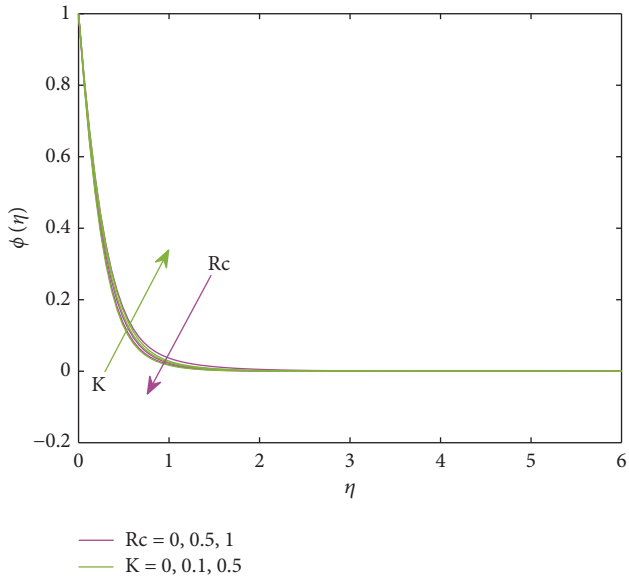

Figure 8: Behavior of Nr and Q on fluid temperature.

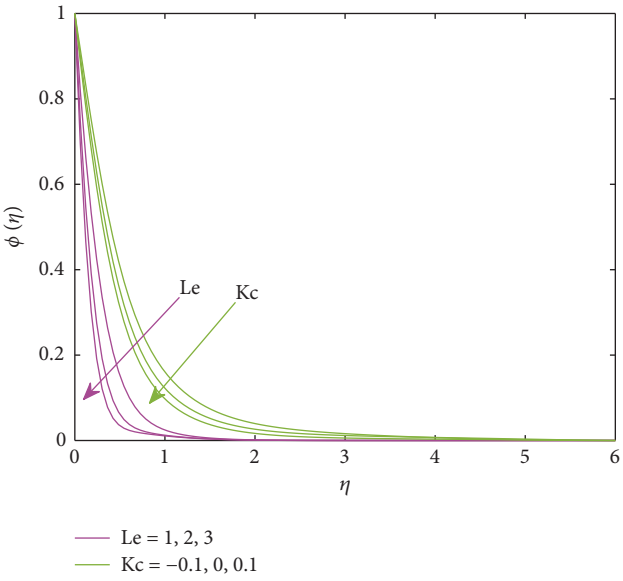

Figure 10: Role of Le and Kc on fluid concentration.

concentration profile, given the existence of the other contributing parameters. The enhanced thermophoresis decelerates the concentration distribution, whereas reverse impact is rendered for the enhanced Brownian motion parameter. Figure 10 elaborates on the dissimilarity of the Lewis number and the chemical reaction affecting the concentration profile. The Lewis number is described as the ratio of the diffusivities, i.e., the thermal diffusion concerning the solutal diffusion. The increasing Lewis number suggests the retardation in the solutal diffusion. Therefore, increasing the Lewis number attenuates the concentration profiles significantly. It is also observed that the inclusion of the chemical ration parameter retards the solutal profile.

The numerical results for the rate constants, i.e., the shear rate, Nusselt, and Sherwood numbers, with the multiple values of the significant limitations, are displayed in Table 2. The observation clarifies that the enhanced values of the viscoelastic parameter and the velocity slip parameter enhance the shear rate, whereas the inclusion of the magnetic parameter along with the thermal and solutal buoyancy parameters decelerate it significantly. The rate of heat transfer of the nanofluid is augmented due to the increasing Prandtl number and the additional heat source and thermal radiation, but the increasing Brownian and thermophoresis retard it at all points within the domain. The Lewis number and the chemical reaction parameter significantly enhance the solutal rate transfer.

Table 2: Computation of rate coefficients.

Rc	K	M	λ_1	λ_2	Pr	Nr	Nb	Nt	Q	Le	Kc	Cf Nu Sh
0.3	0.5	1	0.5	0.5	7	0.5	0.5	0.01	0.1	1	1	−1.5539 0.1385 3.2001
0.5												−2.6057 0.1586 3.2573
0.3	0.1											−2.8625 0.1934 3.3587
	0.2											−2.3708 0.1751 3.3044
	0.5	2										−1.7338 0.1054 3.1403
		3										−1.8608 0.0776 3.0941
		1	0.1									−1.6583 0.1206 3.1661
			0.2									−1.6312 0.1255 3.1753
			0.5	0.1								−1.5964 0.1332 3.1881
				0.2								−1.5857 0.1346 3.1911
				0.5	0.7							−1.4093 0.2745 1.1694
					2							−1.4637 0.3099 1.6671
					7	0.1						−1.5613 0.0645 3.2098
						0.2						−1.5594 0.0851 3.2072
						0.5	0.1					−1.6650 1.2139 3.1028
							0.2					−1.6615 0.8213 3.1938
							0.5	0.1				−1.5436 0.1245 3.7359
								0.2				−1.5324 0.1084 4.3457
								0.01	0.1			−1.5539 0.1385 3.2001
									0.2			−1.5464 0.0470 3.2060
									0.5	2		−1.5750 0.1214 4.5928
										3		−1.5854 0.1162 5.6782
										1	−1	−0.1204 −401.2223 −3.5864
											0	−1.6096 0.3284 1.6550
											1	−1.5539 0.1385 3.2001

6. Conclusion

The present study analyzes the analytical and numerical investigation hybridisation for the free convection of the viscoelastic nanofluid flow past a vertical stretching surface. The cross-diffusion between the concentration and temperature gradient profiles corresponding to Brownian thermophoresis enriches the study. Considering the thermal radiation and the chemical reaction also greatly enhance the physical properties of the thermal and solutal profiles. The significant behaviour of the several parameters is presented and described briefly. However, the measure contribution of important parameters is described as follows:

(i) The correlation between the numerical results of the heat transfer rate for the particular values shows the validation of the present work and also provides the convergence criteria of the profiles obtained by using the current methodologies.

(ii) The contribution of the non-Newtonian fluid due to the interaction of the elastic parameter encourages the enhancement of the fluid velocity near the surface region; however, reverse impact is observed far away from the sheet, but this variation is insignificant.

(iii) The enhanced velocity slip retards the fluid velocity, whereas the inclusion of solutal and thermal buoyancy parameters overshoots the nanofluid velocity profiles.

(iv) Random motion of the particles within the flow domain enhances the fluid temperature, and the thermophoresis significantly retards it, but the reverse trend is marked in the fluid concentration profiles.

(v) The decelerating effect of the solutal diffusion occurs in a significant rise in the Lewis number. Therefore, the fluid concentration attenuates throughout the domain. The inclusion of chemical reactions also significantly decelerates the fluid concentration.

(vi) The elasticity parameter and the magnetic parameter's inclusion favour a significant increment in the shear rate. The increasing Prandtl number and the thermal radiation also enhance the heat transfer rate. It is also observed that solutal rate transfer also enhances the significant increase in the Lewis number.

Finally, the present paper not only describes the parametric behaviour of the physical constraints on the flow phenomena but also provides significant contributions of these parameters to the enhancement of heat transport phenomena that will be beneficial in several sectors like industrial applications, physiological studies, biomedical areas, etc. Furthermore, one can redesign the Tiwari-Das model so that the use of nanoparticles plays an important role in enhancing heat transport phenomena. Moreover, the governing equations can be handled by adopting approximate analytical techniques like the Adomian Decomposition

Method, Homotopy Perturbation Method, Variation Parameter Method, etc.

Data Availability

All the relevant data are included in the manuscript.

Conflicts of Interest

The authors declare that there are no conflicts of interest.

References

[1] U. S. S. Choi, "Enhancing thermal conductivity of fluids with nanoparticles," *FED – ASME Fluids Eng. Div.Newsl,* vol. 231, pp. 99–105, 1995.

[2] H. S. Takhar, A. J. Chamkha, and G. Nath, "Flow and mass transfer on a stretching sheet with a magnetic field and chemically reactive species," *International Journal of Engineering Science*, vol. 38, no. 12, pp. 1303–1314, 2000.

[3] N. A. Azim and M. K. Chowdhury, "MHD-conjugate free convection from an isothermal horizontal circular cylinder with Joule heating and heat generation," *Journal of Computational Methods in Physics*, vol. 2013, pp. 1–11, 2013.

[4] B. C. Parida, B. K. Swain, N. Senapati, and S. Sahoo, "Viscous dissipation effect on MHD free convective flow in the presence of thermal radiation and chemical reaction," *Mathematical Modelling of Engineering Problems*, vol. 7, no. 3, pp. 387–394, 2020.

[5] R. M. Ramana, V. Raju, and J. G. Kumar, "Multiple slips and chemical reaction effects on unsteady MHD heat and mass transfer flow over a permeable stretching sheet with radiation," *Turk J Comput Math educ*, vol. 12, no. 6, pp. 4489–4498, 2021, https://turcomat.org/index.php/turkbilmat/article/view/8435.

[6] S. T. Suganya, P. Balaganesan, L. Rajendran, and M. Abukhaled, "Analytical discussion and sensitivity analysis of parameters of magnetohydrodynamic free convective flow in an inclined plate," *Eur J Pure Appl Math*, vol. 13, no. 3, pp. 631–644, 2020.

[7] M. N. Uddin, M. A. Alim, and M. M. K. Chowdhury, "Effects of mass transfer on MHD mixed convective flow along inclined porous plate," *Procedia Engineering*, vol. 90, pp. 491–496, 2014.

[8] K. Sarada Bs, "The effect of chemical reaction on an unsteady MHD free convection flow past an infinite vertical porous plate with variable suction," *Ijmer*, vol. 3, no. 2, pp. 725–735, 2013.

[9] G. S. Seth, A. Bhattacharyya, and R. Tripathi, "Effect of hall current on MHD natural convection heat and mass transfer flow of rotating fluid past a vertical plate with ramped wall temperature," *Frontiers in Heat and Mass Transfer*, vol. 9, 2017.

[10] P. Satya Narayana, B. Venkateswarlu, and B. Devika, "Chemical reaction and heat source effects on MHD oscillatory flow in an irregular channel," *Ain Shams Engineering Journal*, vol. 7, no. 4, pp. 1079–1088, 2016.

[11] G. Ramana Reddy, N. Bhaskar Reddy, and R. S. R. Gorla, "Radiation and chemical reaction effects on MHD flow along a moving vertical porous plate," *International Journal of Applied Mechanics and Engineering*, vol. 21, no. 1, pp. 157–168, 2016.

[12] N. Ahmed and K. K. Das, "Chemical reaction effect on MHD free convective mass transfer flow past an impulsively started vertical plate," *Int J Heat Technol*, vol. 32, no. 1-2, pp. 15–22, 2014.

[13] K. V. S. Raju, T. Sudhakar Reddy, M. C. Raju, P. Satya Narayana, and S. Venkataramana, "MHD convective flow through porous medium in a horizontal channel with insulated and impermeable bottom wall in the presence of viscous dissipation and Joule heating," *Ain Shams Engineering Journal*, vol. 5, no. 2, pp. 543–551, 2014.

[14] H. Mondal, D. Pal, S. Chatterjee, and P. Sibanda, "Thermophoresis and Soret-Dufour on MHD mixed convection mass transfer over an inclined plate with non-uniform heat source/sink and chemical reaction," *Ain Shams Engineering Journal*, vol. 9, no. 4, pp. 2111–2121, 2018.

[15] H. S. U. Sehra, S. U. Haq, S. I. A. Shah, K. S. Nisar, S. U. Jan, and I. Khan, "Convection heat mass transfer and MHD flow over a vertical plate with chemical reaction, arbitrary shear stress and exponential heating," *Scientific Reports*, vol. 11, no. 1, pp. 4265–4311, 2021.

[16] T. M. Agbaje and P. G. L. Leach, "A numerical examination of an unsteady nonlinear MHD flow in the presence of thermal radiation and heat generation," *International Journal of Applied Mechanics and Engineering*, vol. 26, no. 1, pp. 1–17, 2021.

[17] N. A. Khan and F. Naz, "Three dimensional flow and mass transfer analysis of a second grade fluid in a porous channel with a lower stretching wall," *International Journal of Applied Mechanics and Engineering*, vol. 21, no. 2, pp. 359–376, 2016.

[18] K. Rajagopal, P. H. Veena, and V. K. Pravin, "Unsteady three-dimensional mhd flow due to impulsive motion with heat and mass transfer past a stretching sheet in a saturated porous medium," *Ijame*, vol. 18, no. 1, pp. 137–151, 2013.

[19] P. K. Pattnaik, S. R. Mishra, and R. P. Sharma, "Numerical simulation for flow through conducting metal and metallic oxide nanofluids," *Journal of Nanofluids*, vol. 9, no. 4, pp. 354–361, 2020.

[20] P. K. Pattnaik, S. R. Mishra, B. Mahanthesh, B. J. Gireesha, and M. Rahimi-Gorji, "Heat transport of nano-micropolar fluid with an exponential heat source on a convectively heated elongated plate using numerical computation," *Multidiscipline Modeling in Materials and Structures*, vol. 16, no. 5, pp. 1295–1312, 2020.

[21] P. K. Pattnaik, S. Mishra, and M. M. Bhatti, "Duan–rach approach to study Al2O3-ethylene glycol $C_2H_6O_2$ nanofluid flow based upon KKL model," *Inventions*, vol. 5, no. 3, pp. 45–23, 2020.

[22] S. Jena, S. R. Mishra, and P. K. Pattnaik, "Development in the heat transfer properties of nanofluid due to the interaction of inclined magnetic field and non-uniform heat source," *Journal of Nanofluids*, vol. 9, no. 3, pp. 143–151, 2020.

[23] P. K. Pattnaik, S. R. Mishra, A. K. Barik, and A. K. Mishra, "Influence of chemical reaction on magnetohydrodynamic flow over an exponential stretching sheet, A numerical study," *International Journal of Fluid Mechanics Research*, vol. 47, no. 3, pp. 217–228, 2020.

[24] A. K. Barik, S. K. Mishra, S. R. Mishra, and P. K. Pattnaik, "Multiple slip effects on MHD nanofluid flow over an inclined, radiative, and chemically reacting stretching sheet by means of FDM," *Heat Transfer - Asian Research*, vol. 49, no. 1, pp. 477–501, 2020.

[25] P. K. Pattnaik, S. Jena, A. Dei, and G. Sahu, "Impact of chemical reaction on micropolar fluid past a stretching sheet," *JP Journal of Heat and Mass Transfer*, vol. 18, no. 1, pp. 207–223, 2019.

[26] B. Mohanty, S. Jena, and P. K. Pattnaik, "MHD nanofluid flow over stretching/shrinking surface in presence of heat radiation using numerical method," *International Journal on Emerging Technologies*, vol. 10, no. 2, pp. 119–125, 2019.

[27] S. R. Mishra, P. K. Pattnaik, M. M. Bhatti, and T. Abbas, "Analysis of heat and mass transfer with MHD and chemical reaction effects on viscoelastic fluid over a stretching sheet," *Indian Journal of Physics*, vol. 91, no. 10, pp. 1219–1227, 2017.

[28] S. R. Mishra, P. K. Pattnaik, and G. C. Dash, "Effect of heat source and double stratification on MHD free convection in a micropolar fluid," *Alexandria Engineering Journal*, vol. 54, no. 3, pp. 681–689, 2015.

[29] P. K. Pattnaik and T. Biswal, "Analytical solution of MHD free convective flow through porous media with time-dependent temperature and concentration," *Walailak Journal of Science and Technology*, vol. 12, no. 9, pp. 749–762, 2015.

[30] R. Biswas, M. S. Hossain, R. Islam, S. F. Ahmmed, S. R. Mishra, and M. Afikuzzaman, "Computational treatment of MHD Maxwell nanofluid flow across a stretching sheet considering higher-order chemical reaction and thermal radiation," *Journal of Computational Mathematics and Data Science*, vol. 4, Article ID 100048, 2022.

[31] H. Zeb, S. Bhatti, U. Khan, H. A. Wahab, A. Mohamed, and I. Khan, "Impact of homogeneous-heterogeneous reactions on flow of non-Newtonian ferrofluid over a stretching sheet," *Journal of Nanomaterials*, pp. 1–11, 2022.

[32] K. Javid, M. Ellahi, K. Al-Khaled et al., "Case studies in Thermal Engineering, EMHD creeping rheology of nanofluid through a micro-channel via ciliated propulsion under porosity and thermal effects," vol. 30, Article ID 101746, 2022.

[33] A. Aldabesh, A. Haredy, K. Al-Khaled, S. U. Khan, and I. Tlili, "Darcy resistance flow of Sutterby nanofluid with microorganisms with applications of nano-biofuel cells," *Scientific Reports*, vol. 12, no. 1, p. 7514, 2022.

[34] A. Raza, H. A. Hejazi, S. U. Khan, M. I. Khan, K. Smida, and I. Tlili, "Unsteady incompressible flow of magnetized aluminium oxide and titanium oxide nanoparticles with blood base fluid," *Journal of the Indian Chemical Society*, vol. 99, no. 7, Article ID 100568, 2022.

[35] S. U. Khan, K. Al-Khaled, A. Aldabesh, M. Awais, and I. Tlili, "Bioconvection flow in accelerated Couple stress nanoparticles with activation energy: bio-fuel applications," *Scientific Reports*, vol. 11, no. 1, p. 3331, 2021.

[36] F. Haq, M. I. Khan, E. M. El-Zahar, S. U. Khan, S. Farooq, and K. Guedri, "Theoretical investigation of radiative viscous hybrid nanofluid towards a permeable surface of cylinder," *Chinese Journal of Physics*, vol. 77, pp. 2761–2772, 2022.

[37] K. A. M. Alharbi, I. B. Mansir, K. Al-Khaled et al., "Heat transfer enhancement for slip flow of single-walled and multi-walled carbon nanotubes due to linear inclined surface by using modified Prabhakar fractional approach," *Archive of Applied Mechanics*, vol. 92, no. 8, pp. 2455–2465, 2022.

[38] F. S. Khan, M. Khalid, O. Bazighifan, and A. El-Mesady, "Euler's numerical method on fractional DSEK model under ABC derivative," *Complexity*, vol. 2022, Article ID 4475491, 2022.

[39] M. Higazy, A. El-Mesady, A. M. S. Mahdy, S. Ullah, and A Al-Ghamdi, "Numerical, approximate solutions, and optimal control on the deathly lassa hemorrhagic fever disease in pregnant women," *Journal of Function Spaces*, vol. 2021, pp. 1–15, 2021.

[40] W. A. Khan and I. Pop, "Boundary-layer flow of a nanofluid past a stretching sheet," *International Journal of Heat and Mass Transfer*, vol. 53, no. 11-12, pp. 2477–2483, 2010.

[41] R. S. Reddy Gorla and I. Sidawi, "Free convection on a vertical stretching surface with suction and blowing," *Applied Scientific Research*, vol. 52, no. 3, pp. 247–257, 1994.